



ISTITUTO NAZIONALE DI RICERCA METROLOGICA Repository Istituzionale

The LISA interferometer: impact of stray light on the phase of the heterodyne signal

This is the author's accepted version of the contribution published as:

Original

The LISA interferometer: impact of stray light on the phase of the heterodyne signal / Sasso, C P; Mana, G; Mottini, S. - In: CLASSICAL AND QUANTUM GRAVITY. - ISSN 0264-9381. - 36:7(2019), p. 075015.
[10.1088/1361-6382/ab0a15]

Availability:

This version is available at: 11696/62219 since: 2020-09-01T14:30:22Z

Publisher:

IOP

Published

DOI:10.1088/1361-6382/ab0a15

Terms of use:

This article is made available under terms and conditions as specified in the corresponding bibliographic description in the repository

Publisher copyright

Institute of Physics Publishing Ltd (IOP)

IOP Publishing Ltd is not responsible for any errors or omissions in this version of the manuscript or any version derived from it. The Version of Record is available online at DOI indicated above

(Article begins on next page)

The LISA interferometer: impact of stray light on the phase of the heterodyne signal

C P Sasso¹, G Mana¹, and S Mottini²

¹INRIM – Istituto Nazionale di Ricerca Metrologica, Str. delle cacce 91, 10135 Torino, Italy

²Thales Alenia Space, Str. Antica di Collegno, 253, 10146 Torino, Italy

E-mail: c.sasso@inrim.it

Abstract. The Laser Interferometer Space Antenna is a foreseen gravitational wave detector, which aims to detect 10^{-20} strains in the frequency range from 0.1 mHz to 1 Hz. It is a triangular constellation, with equal sides of 2.5×10^9 m, of three spacecraft, where heterodyne interferometry measures the spacecraft distances. The stray light from the powerful transmitted beam can overlap with the received one and interfere with the heterodyne signal. We investigated the contribution of random phase variations of the stray photons to the noise of the heterodyne signal. A balanced detection scheme more effectively mitigates this adverse effect than a separation of the frequencies of the transmitted and local radiation. In the balanced scheme, in order to limit the phase noise to picometer level, the incoherent power of the stray light must be kept below about 10 nW/W for an asymmetry of the recombination beam splitter of 1%.

Submitted to: *Classical and Quantum Gravity*

PACS numbers: 07.60.Ly, 68.49.-h, 04.80.Nn, 95.55.Ym

1. Introduction

The Laser Interferometer Space Antenna (LISA) is a concept for a space-based gravitational wave detector of the European Space Agency. It is a constellation of three spacecrafts – an equilateral triangle with side length of 2.5×10^6 km – trailing the Earth by 20 degrees. It aims to measure the fluctuations of the distance between free-falling masses placed inside the spacecrafts to picometre resolution in the frequency range from 0.1 mHz to 0.1 Hz. The detection of the test mass motions *vs.* the associated optical benches and the phase-linking of the local and remote benches by heterodyne interferometry split the measurement of the test-mass separation into onboard and inter-spacecraft interferometric measurements [1, 2, 3, 4].

To measure their distance, each spacecraft hosts two 30 cm telescopes, which simultaneously transmit and receive the interferometer beams and act as afocal beam expanders having a magnification of about $135\times$. For the transmission, it takes a 2 mm beams and send a collimated beam having a waist diameter of about 30 cm. For the reception, it collects the light from the far spacecraft and reduces it to a 2 mm beam. In both cases, it operates between a pair of conjugate pupils mapping rotations

in the sky into rotations in the optical bench, ideally without transverse motions and length changes.

The telescopes are fed by stabilised 1064 nm lasers delivering 2 W of optical power, which leads to a far-field received power of about 700 pW at the 30 cm entrance-aperture of the receiving telescope [5, 6]. As shown in Fig.1, the phase of the weak received beam is detected by interfering it with a local reference, e.g., a fraction of the transmitted beam, about 2 mW. Since both the transmission and reception are carried out by the same telescope and the same optical bench accommodates both the onboard and inter-spacecraft interferometers, the transmitted and received beams share part of their optical path [7]. Consequently, although measures are taken to mitigate its detrimental effects, the light backscattered from the powerful transmitted beam into the received one interferes with the measurement of the spacecraft distance and might jeopardise the sought picometer sensitivity [8].

Stray light is not a problem per se, but its phase stability in the measurement bandwidth is. Since it records their movements, any displacement of the backscattering elements causes a noise. The measurement suffers from the light coherently backscattered by the telescope (because of longitudinal displacements from the optical bench) rather than from the optics on optical bench (because of the high dimensional stability required). Measures were proposed to mitigate the impact of stray light, such as tilted optical elements, baffling, off-axis telescopes, polarisation encoding interferometry [9, 10]. Also, measurement strategies, like the use of a balanced receiver [11, 12] and the swap of the local references between the two inter-spacecraft interferometers [3], were investigated.

Experimental observations and an explaining model of the impact of back-reflected light on interferometric measurements are given in [13, 14]. In previous papers, we investigated the phase noise of the inter-spacecraft interferometer due to the coupling of aberrated wavefronts with the transmitter and receiver jitters [15, 16]. In this paper, we estimate the contribution of back-reflected light.

In section 2, we model the interference of stray light with the received and local beams and derive the measurement equations of the phase of the heterodyne signal for both the balanced signal-detection [11, 12] and the swap of the local references [3]. Hence, we quantify how the measurement error depends on the stray-light power, asymmetry of the recombination beam-splitter, motion of the back-scattering elements, and frequency and phase of the received signal. Eventually, section 3 estimates the constraints of the back-scattered power necessary to ensure the targeted picometer resolution.

2. Stray light interference

2.1. Balanced detection

As shown by the Fig.1, the phase ϕ of the received wavefront (the green beam entering the telescope primary mirror) is measured – via optical heterodyne – by interference with a fraction of the beam from the laser source, which acts as a local reference (the orange beam spilled by the first polarizing beam-splitter). The beam transmission and reception are carried out by the same telescope, and the same bench accommodates both the transmission and reception optics. Therefore, the transmitted and received beams share some of the optical elements and some of the launched photons is sent back along the axis of the received beam (the orange wave strolling back up

to the detectors), interfere with it, and contribute to the phase of the heterodyne signal. Since it senses the motion of the scattering elements, the backscattered light increases the measurement noise through its overall amplitude and phase stability in the measurement bandwidth.

A balanced detection of the heterodyne signal, where the beat notes in both output ports of the recombination beam splitter are detected and subtracted, can be applied to overcome this noise [11, 12]. In fact, since the signals of interest are in opposition while the parasitic ones are in phase, the subtraction rejects the noise stemming from the stray light.

We model the stray light reaching the recombination beam splitter by the coherent sum of N coaxial parasitic-rays,

$$u\sqrt{2I_0}e^{i(\omega_1 t + \psi)} = \sqrt{2I_0} \sum_{n=1}^N u_n e^{i\omega_1 t + \psi_n}, \quad (1)$$

where ω_1 is the angular frequency of the transmitted beam, u_n^2 and ψ_n are the fractional power and phase of the parasitic optical fields, whereas $u^2 = |\sum u_n \exp(i\psi_n)|^2$ and $\psi = \arg[\sum u_n \exp(i\psi_n)]$ are those of their coherent sum. **Figure 2 shows the interfering optical fields. It brings into light that the maximizing of the intensity of the local reference (the orange arrow) reduces the impact of the stray light.**

For later convenience, we indicate by $I_{\text{ref}} = 2I_0 \approx 2$ mW the power of the local reference, which is a fraction of the transmitted beam, by $I_{\text{RX}} = a^2 I_{\text{ref}} \approx 700$ pW the received power, and by $a^2 \approx 3.5 \times 10^{-7}$ its fraction to I_{ref} . The total coherent power of the backscattered light, $u^2 I_{\text{ref}}$ is assumed to be much less than I_{ref} and, consequently, $u^2 \ll 1$. In section 3.1, this assumption will be proved consistent with the upper bound imposed by the sought picometre noise level. Therefore, in the following perturbative analysis, only the lowest order contributions to the signal phase of the (dimensionless) fractional power u will be considered.

The parasitic rays interfere with the local reference, $\sqrt{2I_0}e^{i\omega_1 t}$, and the light received from the remote spacecraft, $a\sqrt{2I_0}e^{i\omega_3 t + \phi}$, where ω_1 is the angular frequency of the transmitted beam, ω_3 is the angular frequency of the received beam, and ϕ is the phase of the received wavefront. The total field at output ports of the recombination beam splitters are

$$E_1 = 1 + a_1 e^{i(\Omega_a t + \phi + \pi/2)} + u_1 e^{i(\psi + \pi/2)}, \quad (2a)$$

$$E_2 = e^{i\pi/2} + a_2 e^{i(\Omega_a t + \phi)} + u_2 e^{i\psi}, \quad (2b)$$

where $i = 1, 2$ labels the output ports, $\Omega_a = \omega_3 - \omega_1$ is the heterodyne frequency, $a^2 = a_1^2 + a_2^2 \ll 1$, $u^2 = u_1^2 + u_2^2 \ll 1$, and we omitted the common factor $\sqrt{I_0}e^{i\omega_1 t}$.

The heterodyne signals are

$$S_1(t) = 1 + a_1^2 + u_1^2 - 2u_1 \sin(\psi) - 2a_1 \sin(\Omega_a t + \phi) + 2a_1 u_1 \cos(\Omega_a t + \phi - \psi), \quad (3a)$$

$$S_2(t) = 1 + a_2^2 + u_2^2 + 2u_2 \sin(\psi) + 2a_2 \sin(\Omega_a t + \phi) + 2a_2 u_2 \cos(\Omega_a t + \phi - \psi). \quad (3b)$$

The foreseen measurement of ϕ is based on a digital phase-locked loop [1, 2, 17]. After the signal difference $S_2(t) - S_1(t)$ is anti-aliasing filtered, the digitised signal is multiplied with a local oscillator. The integrated output – which is proportional to the phase difference between the signal and oscillator – is used to lock the frequency of the local oscillator to Ω_a . By modelling the phase recovery as

$$\phi_m = \arg \left[\int_0^{2n\pi/\Omega_a} [S_2(t) - S_1(t)] e^{-i\Omega_a t} dt \right], \quad (4a)$$

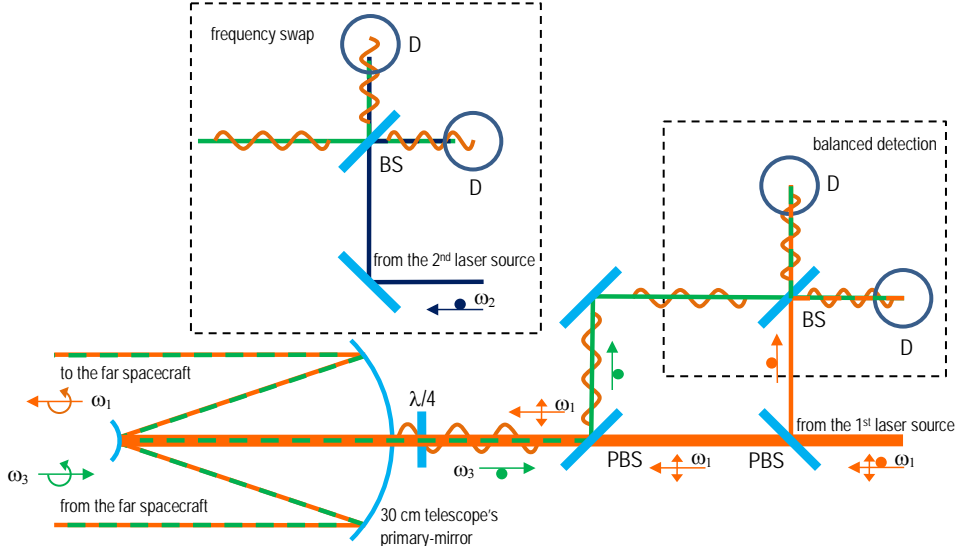


Figure 1. Drawing of the LISA's science interferometer. Though it shows an on-axis telescope layout, an off-axis one is preferred to limit coherent back-reflections. Polarising beam splitters (PBS) separate the transmitted and received light. The received light (angular frequency ω_3) is depicted green; the transmitted light (angular frequency ω_1) is depicted orange; the backscattered light (angular frequency ω_1) is depicted orange waving, the interfering beams are depicted overlapped. The arrows show the beam direction of propagation, whereas the double tip arrows and dots represent the in plane and out of plane polarizations. The "frequency swap" insert shows the beams' recombination when the two spacecrafts primary lasers (operated at angular frequencies ω_1 and ω_2) swap their light. In this case, it substitutes for the "balanced detection" box. BS: recombination beam splitter; D: detectors.

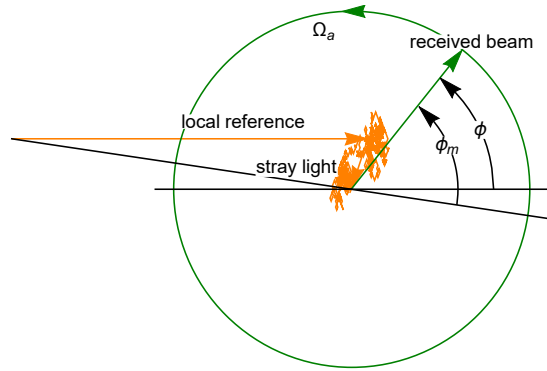


Figure 2. Phasor diagram of the interfering fields. The light from the telescope rotates counterclockwise along the green circle with angular velocity Ω_a . The orange random walk is the stray light. ϕ and ϕ_m are the phases of the received wavefront relative to the local reference and its measured value in the presence of stray light. The difference between ϕ_m and ϕ is the measurement error γ . When the power of the local beam tends to the infinity, the error tends to zero.

where the integration extends over n oscillator cycles, the measurement equation of the heterodyne-signal phase is

$$\phi_m \approx \phi + \pi/2 + \tilde{u} \sin(\psi) + \tilde{u}^2 \sin(\psi) \cos(\psi), \quad (4b)$$

where, since the heterodyne signals are balanced so as to have the same alternating amplitude, $a_1 \approx a_2$ and

$$\tilde{u} = \frac{a_1 u_1 - a_2 u_2}{a_1 + a_2} \approx \frac{u_1 - u_2}{2}. \quad (5)$$

For later convenience, we redefined ψ as $\psi - \pi/2$ and, with the assumption that the fractional stray-light powers $u_{1,2}$ are much smaller than one, we will consider only the terms up to the first order.

If the recombination beam splitter deviates from a 50:50 power-splitting ratio, after adjusting the alternating components of the heterodyne signal in such a way that $a_1 = a_2 = a/\sqrt{2}$, the total coherent-amplitudes of the stray light at the output ports of the interferometers are

$$u_{1,2} = \sqrt{\frac{1 \pm \epsilon}{2}} u \approx \frac{(1 \pm \epsilon/2)u}{\sqrt{2}} \quad (6)$$

where $(1 + \epsilon)/(1 - \epsilon)$ is the ratio of the reflected to the transmitted powers. Hence, the measurement error $\phi_m - \phi$ in (4b),

$$\gamma = \frac{\epsilon u \sin(\psi)}{2\sqrt{2}}, \quad (7)$$

depends on the u^2 ratio between the powers of the backscattered light and local reference and can be made harmless by increasing the last one. The non-balanced detection can be modelled by letting a_1 or a_2 go to zero. In this case,

$$\gamma = \pm u \sin(\psi). \quad (8)$$

2.2. Frequency swap

A different proposal to overcome the stray-light issue is to introduce an offset between the angular frequencies of the local and transmitted beams [3]. This is obtained by swapping the local references between the two spacecraft's optical benches and by operating the two laser sources at different frequencies.

The total field at the interferometer detector is

$$E = 1 + ae^{i(\Omega_a t + \phi)} + ue^{i(\Omega_u t + \psi)}, \quad (9)$$

were $\Omega_a = \omega_3 - \omega_2$ and $\Omega_u = \omega_1 - \omega_2$ are the frequency offsets (*vs.* the local reference) of the received and transmitted beams, respectively. For the sake of simplicity we did not consider a balanced detection and omitted again the $\sqrt{I_0}e^{i\omega_2 t}$ factor, where, now, ω_2 is the (shifted) angular frequency of the local reference. Hence, the heterodyne signal is

$$S(t) = 1 + a^2 + u^2 + 2u \cos(\Omega_u t + \psi) + 2a \cos(\Omega_a t + \phi) + 2au \cos(\Delta_\Omega t + \phi - \psi), \quad (10)$$

where $\Delta_\Omega = \Omega_a - \Omega_u$.

To make it possible the ϕ measurement via a phase-locked loop [1, 2, 17], the fractional power u^2 of the stray-light must be much smaller than that of the received

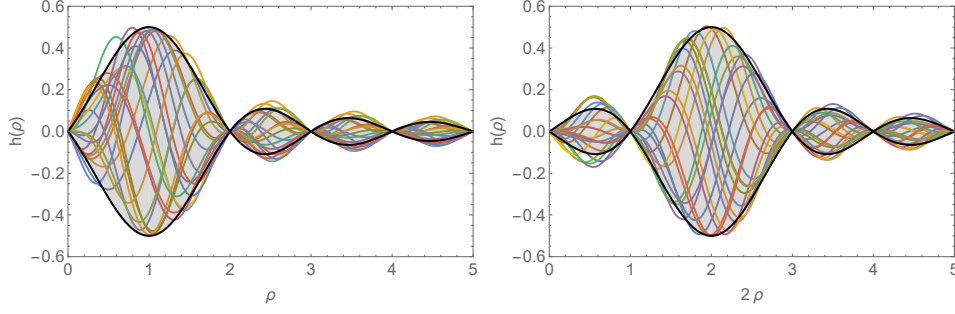


Figure 3. $h(\rho)$ when $n = 1$ (left) and 2 (right). The coloured lines correspond to random values of the received wavefront and stray-light phases. The gray area is the approximate envelope. The fractional power of the local beam is $a^2 = 3.5 \times 10^{-7}$.

beam, a^2 . Hence we assume $u^2/a^2 \ll 1$ and, to the first order in u/a , the phase measurement-equation is

$$\phi_m = \arg \left[\int_0^{2n\pi/\Omega_a} S(t) e^{-i\Omega_a t} dt \right] \approx \phi + \frac{2uh(\rho)}{a}, \quad (11)$$

where

$$h(\rho) = \frac{\sin(n\pi\rho)}{n\pi\rho} \left[\frac{\rho^2 \cos(n\pi\rho + \psi) \sin(\phi)}{1 - \rho^2} - \frac{a(1 - \rho) \cos(n\pi\rho + \psi - \phi) \sin(\phi)}{2 - \rho} \right. \\ \left. + \frac{\rho \sin(n\pi\rho + \psi) \cos(\phi)}{1 - \rho^2} - \frac{a \sin(n\pi\rho + \psi - \phi) \cos(\phi)}{2 - \rho} \right], \quad (12)$$

$\rho = \Omega_u/\Omega_a$, and the integrations were carried out with the aid of Mathematica[®] [18]. The zeroes of $h(\rho)$ occurs at the integer ρ values (both positive and negative) and

$$h(\rho = 0) = -a \sin(\psi)/2, \quad (13)$$

which corresponds to the no swap. Since $a \ll 1$ (actually, $a \approx \sqrt{3.5 \times 10^{-7}}$), the approximate envelope of (12) is

$$|h(\rho)| \lesssim \frac{|\sin(n\pi\rho)|}{2\pi n|1 - \rho|}, \quad (14)$$

which is shown in Fig. 3. The orbital dynamics causes a varying doppler shift and a continuous change, from 2 MHz to 19 MHz, of the heterodyne frequency Ω_a [7]. In turn, the ρ ratio cannot be set to an integer value and the ϕ phase tracks the macroscopic variations of the spacecraft distance. Therefore, we bound the measurement error $\gamma = \phi_m - \phi$ in (11) by the envelope

$$|\gamma| \lesssim \frac{u|\sin(n\pi\rho)|}{\pi a n |1 - \rho|}. \quad (15)$$

It is worth noting that, in order to ensure noise rejection, it is necessary to satisfy the constraint $|n\rho| \gg 1$. Also, contrary to (7), the measurement error depends on the u^2/a^2 ratio between the powers of the backscattered and received lights and is unaffected by the power of the local reference.

3. Phase noise

3.1. Balanced detection

The phases of the parasitic rays $u_n e^{i\psi_n}$ in (1) are unpredictable. Therefore, in order to evaluate their effect on the heterodyne signal, let us assume that the motion of every scattering element is uniformly distributed in the $[-\lambda/2, +\lambda/2]$ interval, where $\lambda = 1064$ nm is the wavelength. A less extremal assumption will be discussed later. Hence,

$$\sin(\psi_n) \sim \frac{1}{\pi \sqrt{1 - z_n^2}}, \quad (16)$$

where the tilde means "is distributed as" and $-1 < z_n < 1$ are the $\sin(\psi_n)$ values. Remembering that

$$u \cos(\psi) + iu \sin(\psi) = u e^{i\psi} = \sum_{n=1}^N u_n \cos(\psi_n) + i \sum_{n=1}^N u_n \sin(\psi_n), \quad (17)$$

we obtain

$$\langle u \sin(\psi) \rangle = \left\langle \sum_{n=1}^N u_n \sin(\psi_n) \right\rangle = 0 \quad (18)$$

and, since $\text{var}[\sin(\psi_n)] = 1/2$,

$$\text{var}[u \sin(\psi)] = \frac{1}{2} \sum_{n=1}^N u_n^2 = \frac{I_{\text{stray}}}{2I_{\text{ref}}}, \quad (19)$$

where $I_{\text{stray}} = (\sum_{n=1}^N u_n^2) I_{\text{ref}}$ is the total incoherent power of the stray light and I_{ref} is the power of the local beam. Therefore, on the average, the phase error (7) is null. Its variance is

$$\sigma_\gamma^2 = \frac{\epsilon I_{\text{stray}}}{4\sqrt{2} I_{\text{ref}}}. \quad (20)$$

The requirement $\sigma_\gamma \lambda / (2\pi) < 1$ pm – or, being $\lambda = 1064$ nm, $\sigma_\gamma / (2\pi) < 10^{-6}$ – constrains the total incoherent-power of the stray light to

$$I_{\text{stray}} \lesssim \frac{2 \times 10^{-10} I_{\text{ref}}}{\epsilon}. \quad (21)$$

Given the otherwise required high stability of the optical assembly, to examine the impact of realistic elements' motions, we assume that the phases ψ_n in (1) are uniformly walking in the intervals $[\psi_{n0} - \alpha, \psi_{n0} + \alpha]$. Since now

$$\text{var}[u_n \sin(\psi_n)] = \frac{\alpha^2 u_n^2 \cos^2(\psi_{0n})}{3} + \mathcal{O}(\alpha^4), \quad (22)$$

up to the second order, (19) must be updated to

$$\begin{aligned} \text{var}[u \sin(\psi)] &= \frac{\alpha^2 \sum_{n=1}^N u_n^2 \cos^2(\psi_{0n})}{3} \\ &\approx \frac{\alpha^2 \sum_{n=1}^N u_n^2}{6} = \frac{\alpha^2 I_{\text{stray}}}{6I_{\text{ref}}}, \end{aligned} \quad (23)$$

where we assumed ψ_{0n} uniformly distributed in the $[-\pi, \pi]$ interval and substituted the $1/2$ average for $\cos^2(\psi_{0n})$. Therefore, the variance of the phase error (7) is

$$\sigma_\gamma^2 = \frac{\epsilon \alpha^2 I_{\text{stray}}}{12\sqrt{2} I_{\text{ref}}}. \quad (24)$$

Consequently, the constrain (21) relaxes to

$$I_{\text{stray}} \lesssim \frac{6 \times 10^{-10} I_{\text{ref}}}{\epsilon \alpha^2}. \quad (25)$$

To give a numerical example, we consider a split-ratio error $\epsilon \approx 10^{-2}$ and a worst-case random walk of the backscattering elements in the $[-\lambda/2, +\lambda/2]$ interval. From (21), to keep the signal noise to within 1 pm, the total incoherent power of the light backscattered into the detector field of view must be constrained to $I_{\text{stray}} \lesssim 2 \times 10^{-8} I_{\text{ref}}$. We also note that this constrain implies $u \lesssim 10^{-4}$, which is consistent with the $u \ll 1$ assumption made.

3.2. Frequency swap

The continuous change of the heterodyne frequency Ω_a and phase ϕ due to the spacecraft's orbit-dynamics makes the phase error in (11) varying also if the scattering elements do not move. By assuming the phase error uniformly distributed within the bounds (15) and averaging the total coherent power of the stray light, the noise variance is bounded by

$$\sigma_\gamma^2 = \frac{1}{3} \frac{\langle u^2 \rangle \sin^2(n\pi\rho)}{\pi^2 a^2 n^2 (1-\rho)^2} = \frac{I_{\text{stray}}}{3\pi^2 n^2 (1-\rho)^2 I_{\text{RX}}}, \quad (26)$$

where $\langle u^2 \rangle = \sum u_n^2$ is the mean total coherent-power of the stray light, $I_{\text{stray}} = (\sum u_n^2) I_{\text{ref}}$ is the total incoherent-power, $I_{\text{RX}} = a^2 I_{\text{ref}}$ is the received power, and we set $\sin^2(n\pi\rho)$ to one.

The sought $\sigma_\gamma \lambda / (2\pi) < 1$ pm target requires that total incoherent-power of the stray light is constrained by

$$I_{\text{stray}} \lesssim 1.2 \times 10^{-9} n^2 (1-\rho)^2 I_{\text{RX}} \approx 4.2 \times 10^{-16} n^2 (1-\rho)^2 I_{\text{ref}}, \quad (27)$$

where we used $I_{\text{RX}} = 3.5 \times 10^{-7} I_{\text{ref}}$.

To give a numerical example, we assume a $\rho = 10$ ratio between the heterodyne frequencies of the transmitted and received signals, the transmitted signal ones the higher. To keep the signal noise to within 1 pm, the total incoherent power of the light backscattered into the detector field of view must be constrained to $I_{\text{stray}} \lesssim 4.2 \times 10^{-14} n^2 I_{\text{ref}}$. Therefore, remembering the $I_{\text{stray}} \lesssim 2 \times 10^{-8} I_{\text{ref}}$ constraint related to the balanced detection, a competitive swap requires at least 10^4 integration cycles. Furthermore, to ensure that the phase-locked oscillator locks to the received signal, it is also necessary that $I_{\text{stray}} \ll I_{\text{RX}}$, which can be relaxed only by increasing the power of the received signal.

4. Conclusions

The separation of the LISA's spacecraft is monitored by heterodyne interferometry down to picometre sensitivity, in which laser beams are transmitted and received by the same telescopes. The phase of the received wavefront is detected by mixing it with a fraction of the transmitted one. The light backscattered from the transmitted beam

into the received one has a detrimental effect on the interferometric measurement and, therefore, it is a critical issue. As long as it has a fixed phase, it does not limit the measurement, but any phase variations cause a noise.

We reported noise estimates for the balanced detection of the heterodyne signal and the swap of the local references and quantified how the noise depends on the stray-light power, asymmetry of the recombination beam-splitter, motion of the back-scattering elements, and frequency and phase of the received signal. These results are of importance to the interferometer design and underpin the specifications for the manufacturing of the inter-spacecraft interferometer and the estimate of the error budget.

With a balanced detection and a 1% recombination asymmetry, to limit the phase noise to picometer level, the incoherent power of the stray light must be kept below about $2 \times 10^{-8} I_{\text{ref}}$, where I_{ref} is the power of the local reference. Hence, a high local-reference power relaxes this request.

The swap of the local references demands that the incoherent power of the stray light is well below the received power. This request is to ensure the locking of the phase-locked oscillator to the received signal. Also, increasing the power of the local-reference does not help. Eventually, the orbit dynamics changes continuously the frequency of the received signal and prevents nullifying the noise sensitivity by optimising the heterodyne frequencies of the transmitted and received beams. Therefore, the integration cycles of the heterodyne signal must be increased, paying the price on the measurement bandwidth.

5. Acknowledgments

This work was funded by the European Space Agency (contract 1550005721, Metrology Telescope Design for a Gravitational Wave Observatory Mission).

References

- [1] ESA 2011 NGO Revealing a hidden Universe: opening a new chapter of discovery Tech. Rep. ESA/SRE(2011)19 ESA
- [2] Jennrich O 2009 *Classical and Quantum Gravity* **26** 153001
- [3] Weise D, Braxmaier C, Gath P, Schulte H R and Johann U 2017 Optical metrology subsystem of the LISA gravitational wave detector *International Conference on Space Optics – ICSO 2006 (Proc. of SPIE vol 10567)* ed Armandillo E, Costeraste J and Karafolas N pp 105670Q1 – 105670Q6
- [4] Weise D, Marenaci P, Weimer P, Berger M, Schulte H R, Gath P and Johann U 2017 Opto-mechanical architecture of the LISA instrument *International Conference on Space Optics – ICSO 2008 (Proc. SPIE vol 10566)* ed Costeraste J, Armandillo E and Karafolas N pp 10566Q1 – 10566Q8
- [5] Danzmann K 2017 LISA Laser Interferometer Space Antenna – A proposal in response to the ESA call for L3 mission concepts Tech. Rep. LISA_L3_20170120 Lisa Consortium
- [6] LISA Instrument Group 2017 LISA Payload Description Document Tech. Rep. ESA-L3-EST-INST-DD-001 ESA
- [7] d’Arcio L, Bogenstahl J, Dehne M, Diekmann C, Fitzsimons E D, Fleddermann R, Granova E, Heinzel G, Hogenhuis H, Killow C J, Perreur-Lloyd M, Pijenburg J, Robertson D I, Shoda A, Sohmer A, Taylor A, Tröbs M, Wanner G, Ward H and Weise D 2017 Optical bench development for LISA *International Conference on Space Optics – ICSO 2010 (Proc. of SPIE vol 10565)* ed Armandillo E, Cugny B and Karafolas N pp 10565 – 10565 – 7
- [8] Canuel B, Genin E, Vajente G and Marque J 2013 *Opt. Express* **21** 10546–10562
- [9] Spector A and Mueller G 2012 *Classical and Quantum Gravity* **29** 205005
- [10] Livas J, Sankar S, West G, Seals L, Howard J and Fitzsimons E 2017 *Journal of Physics: Conference Series* **840** 012015

- [11] Carleton H R and Maloney W T 1968 *Appl. Opt.* **7** 1241–1243
- [12] Fleddermann R, Diekmann C, Steier F, Tröbs M, Heinzl G and Danzmann K 2018 *Classical and Quantum Gravity* **35** 075007
- [13] Fujimoto H, Mana G and Nakayama K 2000 *Japanese Journal of Applied Physics* **39** 2870
- [14] Cavagnero G, Mana G and Massa E 2005 *Review of Scientific Instruments* **76** 053106
- [15] Sasso C P, Mana G and Mottini S 2018 *Classical and Quantum Gravity* **35** 185013
- [16] Sasso C P, Mana G and Mottini S 2018 *Classical and Quantum Gravity* **35** 245002
- [17] Shaddock D, Ware B, Halverson P G, Spero R E and Klipstein B 2006 *AIP Conference Proceedings* **873** 654–660
- [18] Wolfram Research, Inc 2017 Mathematica, Version 11.2 Champaign, IL